frontiers in Forests and Global Change

ORIGINAL RESEARCH
published: 27 November 2018
doi: 10.3389/ffgc.2018.00008

Heat Waves Alter Carbon Allocation and Increase Mortality of Aleppo Pine Under Dry Conditions

Benjamin Birami[1], Marielle Gattmann[1], Arnd G. Heyer[2], Rüdiger Grote[1], Almut Arneth[1] and Nadine K. Ruehr[1]**

[1] Institute of Meteorology and Climate Research–Atmospheric Environmental Research (IMK-IFU), Karlsruhe Institute of Technology, Karlsruhe, Germany, [2] Institute of Biomaterials and Biomolecular Systems–Plant-Biotechnology, University of Stuttgart, Stuttgart, Germany

OPEN ACCESS

Edited by:
Jeffrey M. Warren, Oak Ridge National Laboratory (DOE), United States

Reviewed by:
Josef Urban, Mendel University in Brno, Czechia
Jason Vogel, University of Florida, United States

***Correspondence:**
Benjamin Birami
benjamin.birami@kit.edu
Nadine K. Ruehr
nadine.ruehr@kit.edu

Specialty section:
This article was submitted to Forest Ecophysiology, a section of the journal Frontiers in Forests and Global Change

Received: *10 August 2018*
Accepted: *31 October 2018*
Published: *27 November 2018*

Citation:
Birami B, Gattmann M, Heyer AG, Grote R, Arneth A and Ruehr NK (2018) Heat Waves Alter Carbon Allocation and Increase Mortality of Aleppo Pine Under Dry Conditions. Front. For. Glob. Change 1:8. doi: 10.3389/ffgc.2018.00008

Climate extremes are likely to occur more frequently in the future, including a combination of heat waves and drought. However, the responses of trees to combined stress and their post-stress recovery are not fully understood yet. Therefore, this study investigated the responses of semi-arid *Pinus halepensis* seedlings to moderate drought, heat and combined heat-drought stress, as well as post-stress recovery. The seedlings were grown under controlled conditions and exposed to two 4-days-long heat periods, reaching air temperature maxima of 42°C and vapor pressure deficit (VPD) of 7 kPa. Day- and nighttime canopy gas exchange was measured and differences in shoot and root allocation of non-structural carbohydrate (NSC) compounds (soluble sugars, starch, cyclitols, and carboxylic acids) assessed. Fluorescence parameters, nitrate levels, proline content and shoot water potential (ψ) provided additional indicators for stress severity and recovery performance. During the heat periods, net photosynthesis and stomatal conductance decreased immediately. This decline was modest under well-watered conditions, with transpiration and dark respiration rates remaining high and despite reductions in root NSC content, trees recovered following heat release. This was not the case in the heat-drought treatment, where stress resulted in high mortality rates and the few surviving seedlings showed reduced gas exchange rates and low root NSC content, while leaf nitrate and proline remained elevated even 3 weeks after heat release. Shoot ψ indicated that hydraulic failure was not the reason for mortality in the heat-drought seedlings. Instead, we argue that low transpiration rates, which resulted in needle temperatures >47°C during heat stress (6°C above air temperature) have caused irreversible damage. In summary, it could be demonstrated that heat waves in combination with moderate drought can either result in increased mortality or, if the seedlings survive, in delayed recovery. This highlights the potential of an increase in heat wave temperatures to trigger forest decline in semi-arid regions.

Keywords: carbon allocation, combined stress, cyclitols, extreme heat wave, nitrate, non-structural carbohydrates, proline, recovery

INTRODUCTION

Forest dieback related to climate extremes has been observed in most regions of the world (Allen et al., 2010; Anderegg et al., 2012, 2015). In particular heat waves combined with drought, which are increasing in frequency and duration (Meehl and Tebaldi, 2004; Schär, 2015), could be a major trigger of tree mortality (Williams et al., 2012; Allen et al., 2015), yet our understanding of physiological processes within trees to such extremes is scarce.

Trees tightly regulate stomatal conductance (g_s) to balance water supply and water loss. The close coordination between leaf water potential (ψ) and g_s during drought conditions has been reported manifold (Jarvis, 1976; Burghardt and Riederer, 2003; Ripullone et al., 2007; Klein and Niu, 2014; Anderegg et al., 2018), while the responses of g_s to changes in evaporative demand, particular in combination with high temperatures is less clear. During experimental heat wave conditions, g_s has been found to decline (Tatarinov et al., 2015; Duarte et al., 2016; Ruehr et al., 2016; Drake et al., 2018) or to be not affected (Ameye et al., 2012) or even to increase (Urban et al., 2017a,b). Despite such differences in stomatal responses, most heat wave studies have found transpiration (E) to increase under high soil water content. At first, this seems counterintuitive, but can be explained by increases in evaporative demand, which stimulates E and thus is cooling of the leaf.

Increased E causes water-use efficiency (WUE) to sharply decrease, because photosynthesis typically declines at high temperatures (Ameye et al., 2012; Tatarinov et al., 2015; Duarte et al., 2016; Ruehr et al., 2016; Urban et al., 2017b; Drake et al., 2018), which results in a pronounced carbon-water decoupling during heat waves (Drake et al., 2018). The underlying reasons for the strong decline of photosynthesis under heat stress are manifold and include decreases in g_s (Ruehr et al., 2016), reduced enzymatic activity (Haldimann and Feller, 2004; Rashid et al., 2018), inactivation of integral proteins and increased membrane leakage (Quinn, 1988; Hays et al., 2001; Zhang and Sharkey, 2009; Watson, 2015), or a combination of influences (Duarte et al., 2016). In addition, increased photorespiration (Teskey et al., 2015) and mitochondrial respiration decreases photosynthetic efficiency. Temperature thresholds resulting in permanent photosynthetic and whole-leaf damage are reported to range between 40 and 50°C (Colombo and Timmer, 1992; Hüve et al., 2011; O'sullivan et al., 2017; Niinemets, 2018; Rätsep et al., 2018), whereas the exact threshold depends on species, the duration of exposure, water availability and adaptive metabolic responses.

Besides direct tissues damage, temperature increments affect tree C allocation dynamics (Zhao et al., 2013; Ruehr et al., 2016). Because respiration typically increases with temperature, C loss can become larger than C uptake (Zhao et al., 2013) and NSC reserves in trees may deplete. In addition, shoot-to-root allocation patterns are sensitive to stress. While reduced C transport from shoots to roots under drought conditions has been observed (Ruehr et al., 2009; Zang et al., 2014; Blessing et al., 2015), C allocation toward roots can increase under high temperatures (Blessing et al., 2015). However, it remains unclear how such changes in C allocation may affect the resilience of trees. For example, the formation of specific C compounds, such as proline or sugar alcohols can prevent protein denaturation at high temperatures (Hamilton, 2001; Jaindl and Popp, 2006). The amino acid proline can also act as osmolyte, antioxidative defense and membrane stabilizing molecule (Verbruggen and Hermans, 2008; Szabados and Savouré, 2010). In addition, large NSC reserves will be critical to sustain high respiration rates. This indicates a potentially important role of the primary C metabolism in mitigating long-term damages and hence could influence post-stress recovery. It can be speculated that besides actual tissue damage, the amount of C maintained during stress could also be a driving force of repair mechanisms (Galiano et al., 2017).

Following stress release, the ability of trees to recover from heat waves depends on stress severity, which is directly influenced by heat exposure (Hüve et al., 2011). If heat waves are additionally combined with drought, evaporative cooling is diminished and canopy temperature increases (Scherrer et al., 2011). This should then accelerate stress-induced damage and potentially delays post-stress recovery. Semi-arid regions are at particular risk because air temperatures are already high so that even a slight warming can surpass critical levels, especially when evaporative cooling is low (Rotenberg and Yakir, 2010; Liu et al., 2013). Regeneration in semi-arid forests might especially be jeopardized because seedlings are most vulnerable to desiccation due to low rooting depth (limited water supply) and exposure to particularly high temperatures (Kolb and Robberecht, 1996).

The present study investigates the impacts of high temperatures under well-watered and dry conditions on seedlings of *Pinus halepensis,* originating from one of the driest pine forest plantations in the world, located in the Negev desert (Rotenberg and Yakir, 2010). In this region, short heat waves frequently occur that already affects the forest's carbon and water cycling (Tatarinov et al., 2015). For future conditions, it is expected that temperatures are increasing further and precipitation during winter is decreasing (Giorgi and Lionello, 2008; Tabari and Willems, 2018). Thus, the trees might be pushed beyond their stress tolerance limits and the survival of this unique forest might be at risk. In order to increase understanding of Aleppo pine's responses to expected extreme heat waves we investigated shoot gas exchange, fluorescence parameters, and some primary metabolites in shoots and roots in a greenhouse experiment under controlled environmental conditions. In particular the following research questions were addressed: (1) How does shoot gas exchange and water-use efficiency respond to a simulated heat waves with or without drought and do g_s, photosynthesis and E also depend on vapor pressure deficit? (2) What are the main drivers of metabolite dynamics and do they affect the allocation between shoots and

Abbreviations: A_{net}, light-phase carbon assimilation/net photosynthesis; C, fixed carbon; E, transpiration; E_{day}, light-phase transpiration; g_s, stomatal conductance; NSC, non-structural carbon; Π, osmotic potential; PAR, photosynthetic active radiation; ψ, leaf water potential; R_{dark}, dark respiration; RH, relative air humidity; RSW, relative soil water content; TCA, Tri-carboxylic acid cycle; VPD, vapor pressure deficit; WUE, water-use efficiency; WUEa, apparent water-use efficiency; WUEi, intrinsic water-use efficiency.

roots? (3) Are heat and heat-drought stress responses fully reversible post-stress?

MATERIAL AND METHODS

Plant Cultivation and Initial Pre-treatment Conditions

Pinus halepensis (Miller) seedlings were grown from seeds in a scientific greenhouse facility in Garmisch-Partenkirchen, Germany (732 m a.s.l., 47°28′32.87″N, 11°3′44.03″E). The origin of the seed material is a 50-years-old Aleppo pine plantation in Israel (Yatir forest). Cones of trees were sampled growing in close-proximity to a meteorological station and flux tower (IL-Yat, 650 m a.s.l., 31°20′49.2″N, 35°03′07.2″E). About 2–4 weeks after germination of seedlings in Germany, the seedlings were transferred to 1 L pots each, containing a mixture (2:8) of quartz sand (0.7 and 1–2 mm) and vermiculite (ca. 3 mm) with 2 g of slow-release fertilizer (Osmocote® Exact + TE 3–4 months fertilizer 16-9-12 + 2MgO + TE, Everis International B.V., Heerlen, The Netherlands). Three months before starting the experiment, 7 months-old seedlings were planted in larger pots (2.5 L) containing a mixture of 1:2:1 quartz sand (1–2 mm): quartz sand (Dorsolit 4–6 mm): vermiculite (3 mm) with 6 g of slow-release fertilizer added (Osmocote® Exact + TE 5–6 months fertilizer 15-9-12 + 2MgO + TE). Potted seedlings were irrigated regularly, starting with 0.1 L per week, which was later adapted to meet increased water demand of the growing seedlings to 0.15 L per week.

Seedlings were grown under average light intensity of 693 ± 324 μmol $m^{-2}s^{-1}$ (supplemented by sodium vapor greenhouse lamps, T-agro 400 W, Philips) and temperatures and humidity adapted to 10-years monthly-averaged day and night air temperature and relative humidity measured at the Yatir forest site (see **Table S1**). One month before the start of our experiment, seedlings were gradually acclimated from average daytime temperatures of 18°C (night: 12°C) to 25°C (night: 15°C). This is close to the 10-years average measured at Yatir forest during May, when the occurrence of short heat waves is typically observed (Tatarinov et al., 2015).

Seedlings were assigned randomly either to a control, drought, heat or heat-drought treatment with 30 seedlings per group. To maintain ambient air temperature and relative humidity in the control and drought treatment, while conducting heat waves in the heat and heat-drought treatment, the seedlings were placed in two adjacent, but individually controllable compartments of the greenhouse facility.

Environmental Variables

Air temperature and relative humidity sensors (CS215, Campbell Scientific Inc., Logan, Utah, US, enclosed in aspirated radiation shields type 43502, Young, Traverse City, MI, USA) and photosynthetic active radiation (PAR) (PQS 1, Kipp & Zonen, Delft, The Netherlands) were measured continuously at canopy height in each greenhouse compartment. Carbon dioxide concentration was monitored with a CO_2 probe (GMT 222, Vaisala, Helsinki, Finland). Soil water content was measured automatically in 10 pots per treatment using substrate-specific calibrated probes (10HS, Decagon Devices, Inc., WA, USA). All environmental sensors produced half-hourly data that were recorded with data loggers (CR1000, Campbell Scientific, Inc. USA).

Soil moisture is given as relative soil water content (RSW) as follows:

$$RSW = 100 * \frac{(SWC_{\text{sample}} - SWC_{\text{min}})}{(SWC_{\text{max}} - SWC_{\text{min}})} \quad (1)$$

where SWC_{sample} is the actual volumetric soil water content, SWC_{min} is the minimum volumetric soil water content after drying the soil for 48 h at 60°C. SWC_{max} is the soil water content at maximum water holding capacity, which was about 200 cm^3 L^{-1} (20% v/v) for our substrate.

Experimental Conditions

Aleppo pine seedlings exposed to heat and heat-drought treatments were subjected to two heat periods of 4 days each (April 27th–April 30th and May 7th–May 10th, 2016). We simulated naturally occurring heat waves by a gradual increasing temperature throughout 2 days, reaching a maximum during the following 2 days (Tatarinov et al., 2015). In order to test how projected further temperature increases of 2–6°C in the Mediterranean region (Seneviratne et al., 2012) might affect metabolism and survival of tree seedlings, we chose to set 5°C higher air temperature maxima than have been reported so far (Tatarinov et al., 2015). This resulted in a maximum of 43.1°C during the first heat wave and 42.4°C during the second heat wave. Relative humidity (RH) during the heat waves was kept between 20 and 40%, which is similar to air water content under ambient temperature conditions. This resulted in a pronounced increase of VPD up to 7.5 kPa during the heat periods (**Figures 1A,B**) which corresponds to observations in the Yatir forest (Tatarinov et al., 2015). In total, extreme air temperatures above 40°C and VPD > 6 kPa were maintained for 10 h during the first heat wave and 12 h during the second heat wave. Dark-phase (PAR < 10 μmol $m^{-2}s^{-1}$) temperatures reached 33.0°C during the first- and 32.9°C during the second heat wave with a total exposure time of 13 h above 30°C for each heat wave. Outside light was supplemented by sodium vapor lamps, resulting in an average PAR of 416 ± 105 μmol $m^{-2}s^{-1}$ during the course of the experiment (**Figure 1C**). Irrigation of the seedlings was adapted to maintain targeted soil water availability. During the initial control conditions and during the recovery at the end of the experiment, seedlings were watered to a RSW of 40–50% (about 0.15 L three-times per week), which is similar to the average wet season condition of the Yatir forest site (pers. com. Yakir Preisler). One week before the start of the first heat wave, irrigation was withheld in the drought and heat-drought treatment (for 4 days) until a RSW of about 15% was reached (**Figure 1D**). This RSW was maintained by watering with 0.05 L three-times per week. One week after the end of the second heat period, all plants were irrigated to reach similar RSW conditions of 40–50%.

In order to avoid a possible influence on the seedlings from the location within the greenhouse, the position of the

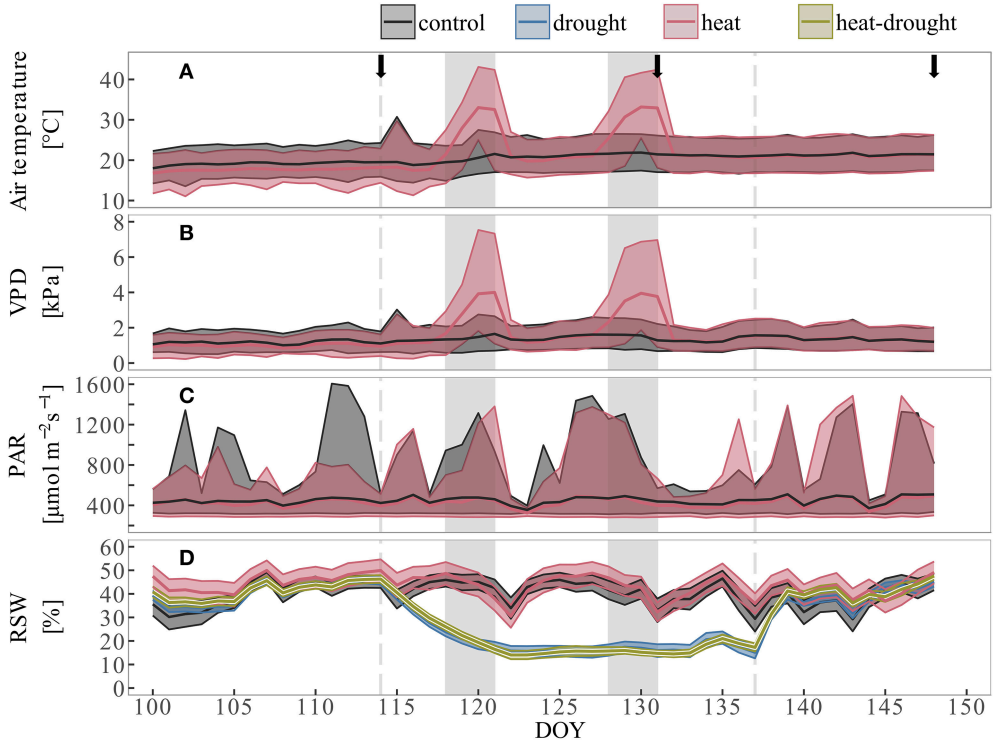

FIGURE 1 | Environmental conditions during the course of the experiment. Shown are **(A)** air temperature, **(B)** vapor pressure deficit and **(C)** photosynthetic active radiation. Colored lines depict daily mean values of two sensors at canopy height (control: black, heat: red), shaded area give daily minimum and maximum values. **(D)** Relative soil water content (rSWC) are treatment averages ($n = 10$) per day. The shaded area is mean ± 1 SE. Dotted lines show begin and end of drought phase, gray shaded areas indicate duration of the two heat waves.

seedlings were changed randomly every 2 weeks during the initial growth phase. During the experimental phase which took place in two separate greenhouse compartments, the seedling position was unchanged because automated shoot cuvettes for gas exchange measurements (see section Gas Exchange Measurements) and soil moisture sensors were permanently installed. During this phase the seedlings were placed spatially interspersed in a randomized block design. Differences in daily-averaged RH between the greenhouse compartments were below 3% (ΔPAR <6%) when heat waves were not applied. Air temperature differences were ∼1°C before the first heat wave and 0.2°C during the remainder of the experiment.

Gas Exchange Measurements

Net photosynthesis (A_{net}), night respiration (R_{dark}) and light phase transpiration (E_{day}) of *Pinus halepensis* shoots were measured with an automated cuvette system (Duarte et al., 2016; Bamberger et al., 2017). Highly UV-transmissive acrylic glass tubes (PMMA Saalberg, 30L: 18W) were placed around tree shoots ($n = 4$ per treatment). The bottom side of each cuvette was sealed by an acrylic glass cap, which allowed the insertion of the seedling. Remaining gaps between tree stem and cap were sealed using plastic putty (Teroson, Düsseldorf, Germany). Each cuvette was supplied with a photodiode for PAR spectrum (G1118, Hamamatsu Photonics, Hamamatsu, Japan) and cross-calibrated with high-precision PAR sensors (PQS 1, Kipp & Zonen, Delft, the Netherlands). For temperature measurements, each cuvette was equipped with a previously calibrated thermocouple (5SC-TTTI-36-2M, Newport Electronics GmbH, Deckenpfronn, Germany). Air mixing within the cuvettes was maintained by a fan (412 FM, ebm-papst GmbH & Co. KG, Mulfingen, Germany). The cuvettes were measured sequentially for 10 min each. After the distal cap had closed automatically, reference air of known CO_2 and H_2O concentration at a rate of 5 L min^{-1} was supplied to the cuvettes. The flow rate was adjusted by a digital mass flow controller (F-201CZ−10K, Bronkhorst, Ruurlo, Netherlands). The measurement air (reference) was generated by an oil-free compressor (SLP-07E-S73, Anest Iwata, Yokohama, Japan) with an Ultra Zero Air generator (Ultra Zero Air GT, LNI Schmidlin SA, Geneva, Switzerland). CO_2 and water vapor (nebulizing evaporation pump, LCU Liquid Calibration Unit, Ionicon, Innsbruck, Austria) was supplied at a constant rate to the air stream, resulting in a CO_2 concentration of 438 ± 3 µmol mol^{-1} and a water vapor concentration of 6.5 ± 0.1 mmol mol^{-1} on average during the experiment.

The slight overpressure that was deliberately generated during each measurement prevented outside air from entering the system. The resulting sample air stream was 1–3 L min^{-1}. Concentration changes between reference and sample air (each provided with 0.5 L min^{-1}) were measured with a

LI-7000, which was connected to a LI-840 (both LI-COR Inc., Lincoln, NE, USA) for absolute concentration measurements of the reference air stream. The sample cells of the two instruments were all supplied with an air stream of 0.5 L min^{-1} each. The LI-840 and LI-7000 were zero and span calibrated before the start of the experiment and the two measurement cells of the LI-7000 were matched on a weekly basis.

As an additional quality check, one cuvette per greenhouse compartment was left empty and allowed detecting any offset between the reference and sample air not caused by plant gas exchange. The concentration differences were small (CO_2: 0.4 [−0.2, 1.2] μmol mol^{-1} in median with lower and upper quartiles; H_2O 0.07 [0.05, 0.12] mmol mol^{-1} with lower and upper quartiles) and were removed by subtraction upon data analysis. After each measurement cycle, the system was flushed with reference air for 1 min. For flux calculation the last 180 s per measurement were used if the following criterion for stability was met: change in $[CO_2] < 0.5$ μmol s^{-1} and change in $[H_2O] < 0.5$ mmol s^{-1}. In total, 94% of the measurements were used for flux calculations.

Gas exchange rates (**Figure 2**) were calculated following an open chamber approach. In brief, (E_{day}) was derived as follows:

$$E_{day} = \frac{\dot{m}\,\Delta W}{\text{Area}_{leaf} * \left(1 - \frac{W_{sample}}{1{,}000}\right)} \quad (2)$$

Where $\dot{m}$ is mass flow [mol s^{-1}] into the cuvettes, ΔW the difference of water vapor in reference- and sample air stream [mol mol^{-1}], W_{sample} the water vapor concentration of the sample air [mol mol^{-1}] and Area_{leaf} [m^2] the half-sided needle area of the shoot.

CO_2 gas exchange fluxes separated into A_{net} and R_{dark} were calculated as:

$$A_{net}(R_{dark}) = -\frac{\dot{m} * \Delta CO_2}{\text{Area}_{leaf}} - \frac{CO_{2\ sample} * E}{1{,}000} \quad (3)$$

With ΔCO_2 as the difference in $[CO_2]$ between reference and sample air stream [mol mol^{-1}], $CO_{2sample}$ carbon dioxide concentration of the sample air stream [mol mol^{-1}].

g_s was calculated as:

$$g_s = \frac{E\left(1{,}000 - \frac{W_{leaf} + W_{sample}}{2}\right)}{W_{leaf} - W_{sample}} \quad (4)$$

$$W_{leaf} = \frac{e_{sat\ leaf}}{p} * 1{,}000 \quad (5)$$

With stomatal conductance g_s in mol $m^{-2}s^{-1}$, saturated vapor pressure of the leaf with $e_{sat\ leaf} = e_{sat}$ in bar and atmospheric pressure p in kPa. Duarte et al. (2016) showed that the ventilation generated by the fans in the cuvettes allowed well air mixing and thus boundary layer for the calculation of g_s could be neglected. In order to determine changes in WUE during heat stress, apparent water-use efficiency WUE_a and intrinsic water-use efficiency WUE_i were derived using the following equations:

$$WUE_a = \frac{A_{net}}{E_{day}} \quad (6)$$

$$WUE_i = \frac{A_{net}}{gs} \quad (7)$$

WUE_a is driven by CO_2 assimilation and water loss at the leaf level, and thus provides a measure for the water cost of carbon fixation. WUE_i provides a measure for leaf physiological changes and is used to characterize photosynthetic efficiency independently of environmental drivers (Bonan et al., 2014; Wieser et al., 2018).

Chlorophyll Fluorescence

A portable photosynthesis system (LI-6400XT, LiCor Bioscience, Lincoln, NE, USA) supplemented with a fluorescence head (6400-40 Leaf Chamber Fluorometer, LiCor Bioscience, Lincoln, NE, USA) was used to measure chlorophyll fluorescence on 4 seedlings per treatment before the start of the treatments, just 1 day after the second heat wave had ended and 3 weeks later during recovery. Measurements were conducted between 9 a.m. and 1 p.m. at a leaf temperature of 25°C and reference $[CO_2]$ of 400 μmol mol^{-1}. Needles were clamped into the leaf cuvette fully covering the cuvette area (2 cm^2). Needles were acclimated to actinic light with optimal PAR (1,200 μmol $m^{-2}s^{-1}$, pre-determined from light response curves) with a blue light proportion of 10% for several min. As soon as changes in fluorescence intensity (F) ceased to values <5, F was considered stable and the measuring sequence was initiated. First, chlorophyll fluorescence at actinic light (F_s') was measured as a steady state value, then needles were briefly exposed to a saturating flash of >7,000 μmol $m^{-2}s^{-1}$ and maximum fluorescence (F_m') was measured. This was followed by a fast switch from actinic light to far red radiation. This so-called dark pulse allowed measurement of minimum chlorophyll fluorescence (F_0'). The photochemical parameters effective photosystem II quantum yield (Φ_{PSII}), maximum light adapted quantum yield of the photosystem II (F_v'/F_m'), coefficients of photochemical fluorescence quenching (qP) and relative electron transfer rate (ETR) were calculated using standard procedures.

Biomass Sampling and Sample Preparation

Entire seedlings were sampled on three occasions during the course of the experiment: pre-stress (April 20th), at the last day of the second heat wave (Mai 10th) and 3 weeks later at the end of the recovery period (Mai 30th). During each sampling campaign, a minimum of six seedlings per treatment (including dead seedlings, see below) were sampled according to a randomized block design. All plant material containing needles above the former cotyledons was assigned as shoot, all plant material below the first roots as root material. Stems were collected but were not used in this study. Additionally, all plant samples were weighted, photographed, and immediately frozen

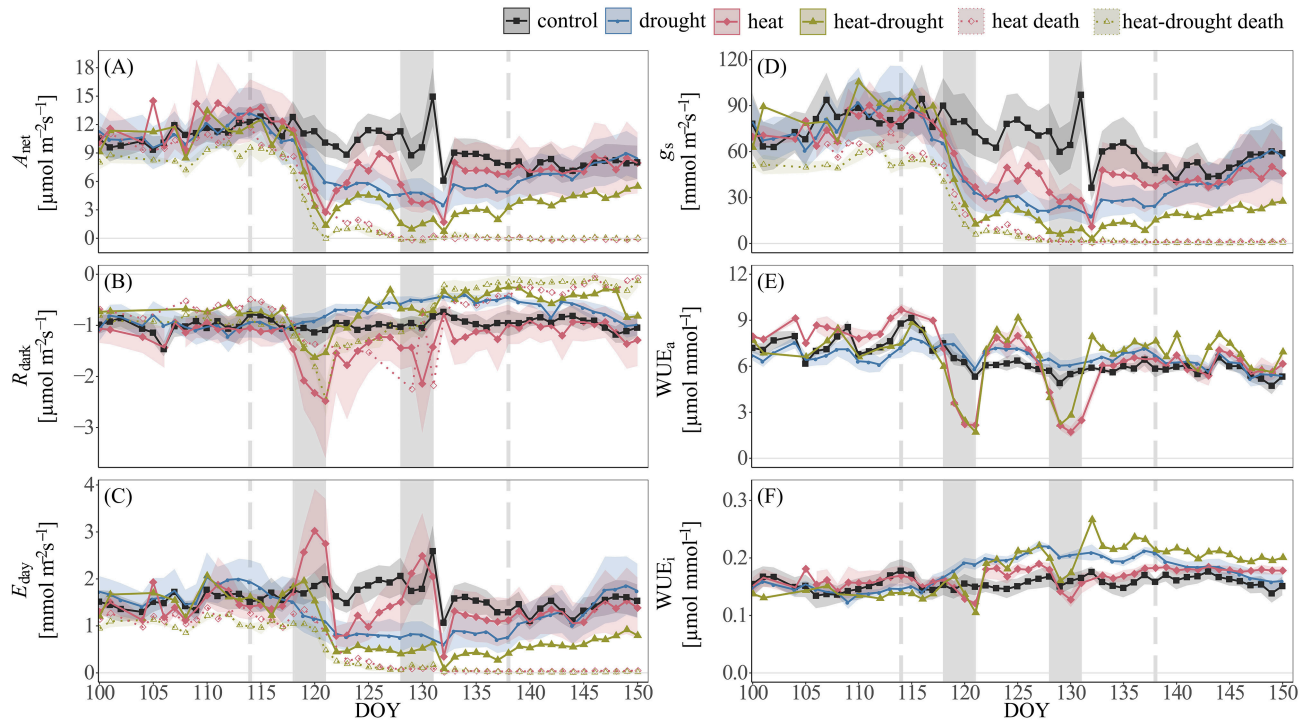

FIGURE 2 | Time-series of shoot gas exchange in *Pinus halepensis* seedlings ($n = 4$ per treatment). Shown are daily averages per treatment of **(A)** net photosynthesis (A_{net}), **(B)** dark respiration (R_{dark}), **(C)** transpiration E, **(D)** stomatal conductance g_S, **(E)** apparent water-use efficiency (WUE_a), and **(F)** intrinsic water-use efficiency (WUE_i). Shoot gas exchange of seedlings that died during the course of the experiment in the heat ($n = 1$) and heat-drought treatment ($n = 3$) is indicated by dotted lines. The shaded areas around the mean represent ±1 SE. The two heat waves are depicted by the light gray areas. The duration of drought is indicated by vertical intermitted lines.

in liquid nitrogen. Time of harvest was between 1 and 2 p.m. Prior to freezing, water potential of shoots (ψ_{shoot}) was measured on some seedlings using a pressure chamber (Model, 600 PMS-Instruments, Albany, OR, USA). Roots and shoots were ground to fine powder in liquid nitrogen with and samples were divided into aliquots and stored at −80°C for further analysis. Dry weight was assessed gravimetrically by drying samples for 48 h at 60°C. In total, 23 control, 22 drought, 28 heat, and 28 heat-drought treated seedlings were sampled. For each sampling campaign metabolites were analyzed in root and shoot tissues and averaged per treatment.

Seedling Mortality

Mortality was determined by two criteria. The first was that foliage appeared dry and had lost most of their greenness (for example see **Figure S1**) while the second criterion was based on absolute shoot water content. In seedlings that looked quite healthy and green, absolute shoot water content was between 58 and 70%, while shoot water content in the other seedlings ranged from 8.2 to 46.7% (**Figure S2**) However, we like to highlight that the decline in shoot water content was unlikely the reason of death (e.g., seedlings of the well-watered heat treatment died as well, but ψ_{shoot} did not indicate water stress in the surviving seedlings, see **Figure 3**), but rather a consequence: after the shoots were permanently damaged and the majority of needles and/or roots no longer functional, water supply ceased and the shoots began to desiccate. The stem desiccation phenomenon was supported by dendrometer data (**Figure S3**). Here, stem dehydration indicated by diameter shrinkage of dying seedlings was observed to occur after the heat waves. Separating between living and dead seedlings was a necessary prerequisite before analyzing the gas exchange and metabolite data.

Analysis of Carbohydrates

Analysis of NSC in shoot and root samples was done following the approach reported by Brauner et al. (2014) based on extraction using boiling ethanol (80%v/v), which was recently defined as standard method for sugar extraction (Quentin et al., 2015). Extracts were analyzed by HPLC (Dionex DX-500 HPLC system, Thermo Scientific) using pulsed amperometric detection by a gold electrode (Dionex ED Au, Thermo Scientific). Soluble sugar compounds (inositol, pinitol, glucose, fructose, sucrose) were separated by a PA1 column (Dionex CarboPac PA−1, Thermo Scientific). Myo-inositol and D-pinitol were co-eluted by our chromatographic method and therefore are referred to cumulative as cyclitols. Glucose, fructose and sucrose are treated together as soluble NSC because single components responded in the same direction to the treatments applied. Remaining extracts were stored at −20°C.

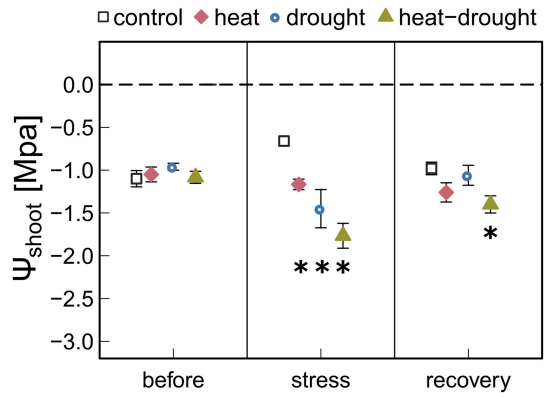

FIGURE 3 | Shoot water potential (ψ_{shoot}) in control, drought, heat, heat-drought trees is given before stress (before), after the second heat wave (stress) and 3 weeks after stress (recovery). The error bars are ±1 SE ($n = 6$, but heat-drought treatment during stress and recovery $n = 3$). Significant treatment effects are given *(ANOVA, $P \leq 0.05$).

Starch extraction was carried out with a modified approach suggested by Hoch et al. (2003). Remaining pellets from soluble sugar extraction were suspended in 1 ml of deionized water (H_2Odd), heated to 95°C for 45 min and then cooled to 30°C before 1 ml of amyloglucosidase reagent (10 mM acetate Buffer pH 4.5, 1 mg ml^{-1} amyloglucosidase) was added. Glucose-oxidase reagent was added containing 2 U ml^{-1} horse radish peroxidase, 5 U ml^{-1} glucose oxidase and 0.1 mg ml^{-1} o-Dianisidin. Samples were kept at 30°C for 2 h, then the reaction was stopped with 5 N HCL and absorption was measured at 540 nm photometrically (Ultrospec 2000 UV/VIS Spectrophotometer, Pharmacia Biotech).

Analysis of carboxylic acids (malic-, fumaric-, citric acid), extracted into hot water, was done as reported by Brauner et al. (2014), again using HPLC (Dionex DX-500 HPLC system, Dionex IonPac AS11-HC, Thermo Scientific) coupled to a suppressor (Dionex AERS 500 Carbonate Electrolytically Regenerated Suppressor, Thermo Scientific) with detection by conductivity (Dionex ED, Thermo Scientific). On the same chromatogram, nitrate, phosphate, sulfate, and chloride were detected as well.

Proline

Proline in shoot and root tissues was analyzed following Rienth et al. (2014). In brief, 25 mg of frozen sample powder was extracted for 10 min in 1 ml H_2Odd at 4°C and centrifuged (13,000 rpm for 15 min). 500 µl of supernatant was added to 500 µl of concentrated Formic acid and vortexed for 5 min. 500 µl of Ninhydrin reagent was added (3% Ninhydrin in Dimethylsulfoxide). Samples were heated (100°C for 15 min) and immediately cooled on ice and then centrifuged (at 13,000 rpm for 1 min). Absorption of the supernatant was measured at 520 nm (Ultrospec 2000 UV/VIS Spectrophotometer, Pharmacia Biotech).

Needle Surface Temperature

Needle surface temperature was measured optically by an infrared camera system (PI 450, Optris, Germany) and analyzed using the manufacturer's software. Recordings were taken at the last day of the second heat wave between 1 and 4 p.m. of at least four individuals per treatment. Air temperature during the measurements was used to correct for background radiation. Emissivity of *P. halepensis* needles was set to 0.97 according to Monod et al. (2009).

Calculation of Osmotic Pressure Potential

Osmotic pressure potential was calculated using the van't Hoff osmotic pressure equation for aqueous mixed electrolyte solvents:

$$\Pi = M*i*R*T \tag{8}$$

where Π is the osmotic pressure potential Pa (kg m^{-1} s^{-1}), M is the molar fraction of all measured osmotic active components (cumulative) including total C, proline, nitrate, sulfate, and phosphate concentrations. R is the ideal gas constant (8.31445 kg m^2 $mol^{-1}K^{-1}s^2$ at standard temperature of 25°C). The van't Hoff factor i represents the degree of dissociation of each solute component. We calculated with fully dissociated solute components for the case that a salt would dissociate into two ions (e.g., $i_{glucose} = 1$, $i_{nitrate} = 2$).

Statistics and Data-Analysis

Treatment effects on metabolite concentrations and differences between treatments were analyzed separately per sampling period (pre-stress, stress and recovery). Analysis of variance (ANOVA) was used to detect treatment effects and a subsequent *post-hoc* test (Tukey's honest significant difference test) was used to reveale differences between treatment groups. Samples that were considered as "dead" were excluded from the analysis. The effect size of treatments compared to the control was calculated as a percent treatment effect (D):

$$D = 100*\frac{(\text{mean}_t - \text{mean}_c)}{\text{mean}_c} \tag{9}$$

where mean_t is the treatment average and mean_c is the average of the control, the standard error (SE) of the treatment effect (D_{SE}) was calculated as follows:

$$D_{SE} = 100*\sqrt{\left(\left(\frac{1}{\text{mean}_c}\right)*SE_t\right)^2 + \left(\left(\frac{\text{mean}_t}{\text{mean}_c{}^2}\right)*SE_C\right)^2} \tag{10}$$

with SE_t and SE_c are the SE of treatments or control. Because shoot gas exchange was measured on the same seedlings throughout the experiments, treatment effects were assessed by application of linear mixed-effects models, which account for the repeated sampling-in-time design. All data processing and statistical analysis was done using R version 3.2.2 (R Core Team, 2015), extended with the "lme4" package (Bates et al., 2015) for linear mixed-effects models.

TABLE 1 | Comparison of needle temperature (T_{needle}) between treatments.

Treatment	T_{needle} [°C]	SE	Δ°C ($T_{needle} - T_{air}$)
Control	28.6	0.63 [$n = 6$]	3.4
Drought	30.7	0.33 [$n = 4$]	5.2
Heat	45.3	0.75 [$n = 6$]	3.1
Heat-drought	47.2	0.57 [$n = 4$]	5.7

Measurements were done using an infrared camera at the end of the second heat wave when air temperature was 40.8–42.1°C in the heat and heat-drought treatment and 25.1–25.4°C in the control and drought treatment. Shown are treatment averages, standard error (±1 SE) and temperature difference between needle and air temperature.

RESULTS

Stress Intensity and Mortality

Heat waves resulted in pronounced death and caused 5 seedlings (23%) in the heat treatment and 15 seedlings (68%) in the heat-drought treatment to die. The surviving seedlings showed only a moderate reduction in ψ_{shoot} (**Figure 3**). Thus, it is unlikely that hydraulic failure was a cause of mortality. However, needle temperatures were affected differently by the treatments. While needle temperatures in the drought and heat-drought treatment were on average 2.6°C higher than in the control and heat treatment (control: +3.4°C above ambient, heat: +3.1°C, drought: +5.2°C, heat-drought: +5.7°C; **Table 1**). Thus, shoots under heat combined with drought had absolute needle temperature >47°C. Although the exact time point of mortality was not investigated in each of the seedlings, the continuous gas exchange measurements pointed to the end of the first heat wave (**Figure 2** intermitted lines) as daytime gas exchange rates did not recover, but declined even further. Shoot R_{dark} reached values close to zero ∼1 week after the end of the last heat wave (**Figure 2C**), which coincides with a halt of the continuous diameter development (**Figure S3**) and indicates that the seedlings were dead. Since the seedlings continued to dry out after death, the shoot water content was below 49% at biomass sampling 2 weeks later, which was in agreement with the death criterion (see Methods section).

Shoot Gas Exchange and Chlorophyll Fluorescence During Stress and Recovery

In the surviving seedlings, large differences in shoot gas exchange were observed between the treatments (see **Table S3** for linear mixed effect model results). While A_{net} and R_{dark} in drought-treated seedlings decreased proportionally (**Figures 2A,B**), we found contrasting responses under high temperature stress. Most markedly, in both the heat and heat-drought treatment a sharp decline in A_{net} was contrasted by a pronounced increase in R_{dark} (heat: +101%, heat-drought: +35%, $P \leq 0.001$) during the first heat wave. In the surviving heat-drought seedling, the increase in R_{dark} during the first heat wave was not observed during the second heat wave and R_{dark} did not reach control levels throughout the remainder of the experiment (−49.8%, $P \leq 0.001$). In contrast, the heat-treated seedlings maintained high R_{dark} rates and A_{net} recovered instantaneously after the second heat wave had ended.

Canopy transpiration was strongly affected by the two heat waves and increased markedly in the heat treatment, while water deficit resulted in a reduction of E_{day} in the heat-drought treatment (**Figure 2C**). In both treatments the changes in E_{day} were accompanied by decreasing g_s (**Figure 2D**). Because A_{net} appeared coupled to g_s but uncoupled from E_{day} during heat wave conditions, WUE_a declined sharply while WUE_i remained relatively unchanged, but slightly increased in the surviving heat-drought seedling post-stress ($P \leq 0.001$; **Figures 2E,F**).

The relationships of shoot gas exchange with VPD (**Figure 4**) revealed striking differences between drought and well-watered seedlings. In the heat treatment, a decline in g_s was particularly visible during the initial increase in VPD (0.5–3 kPa), while g_s remained surprisingly constant at higher VPD. This resulted in increasing E_{day}, while photosynthesis remained constant over a temperature range between 32 and 42°C. The decline of g_s in the heat-drought treatment indicated stomatal closure at a VPD of about 3.5 kPa, tightly limiting E_{day} and A_{net}.

The impairment of the photosynthetic apparatus under heat-drought stress was clearly visible in all measured chlorophyll fluorescence parameters 1 day after the last heat wave (**Figure 5**), where Φ_{PSII} showed a treatment effect (ANOVA, $P \leq 0.001$) and the strongest decline by 78% compared to the control (*post-hoc*, $P \leq 0.001$) and the drought treatment (*post-hoc*, $P \leq 0.05$). The parameters also reflected the reduced, but continuing photosynthetic activity in the heat and drought treatment, in which small but not significant reductions were observed. The apparent recovery of all chlorophyll fluorescence parameters in the heat-drought treatment should be interpreted with caution, because only data of intact needles of the three surviving seedlings are reported.

Non-structural Carbohydrates

We found no distinct stress responses of NSC concentrations in shoots (**Figures 6A,C,E,G**). In contrast, soluble NSC and starch contents in roots declined in response to heat and heat-drought stress (**Figures 6B,D**; see **Tables S4, S5**). Heat-drought caused a steep depletion of soluble sugars (−97%, 2.4 μmol gDW^{-1}) and starch (−98%, 0.8 μmol gDW^{-1}). Carboxylic acids and cyclitols were also significantly affected by heat-drought stress, causing an overall treatment effect (ANOVA, $P \leq 0.001$) and reduction in total C of 83% compared to the control. The Heat-drought treatment differed from all other treatments (*post-hoc*, $P \leq 0.05$).

During recovery, carboxylic acids (toward control and drought) and cyclitols (toward all treatments) increased significantly in shoots of heat-drought treated seedlings (**Figures 6E,G**; *post-hoc*, $P \leq 0.05$). While in the heat and in the heat-drought treatment root soluble NSC and starch increased during recovery close to control values (**Figures 6B,D**), total C remained reduced in the heat-drought treatment (−85%, ANOVA, $P \leq 0.001$). In dying seedlings, NSC contents did not recover (**Figure 6**) and starch storage in shoots and roots was close to depletion.

Proline, Nitrate, and Osmotic Potential

Concentrations increased in shoots of heat and heat-drought treated seedlings during stress and recovery (**Figures 7A,B**)

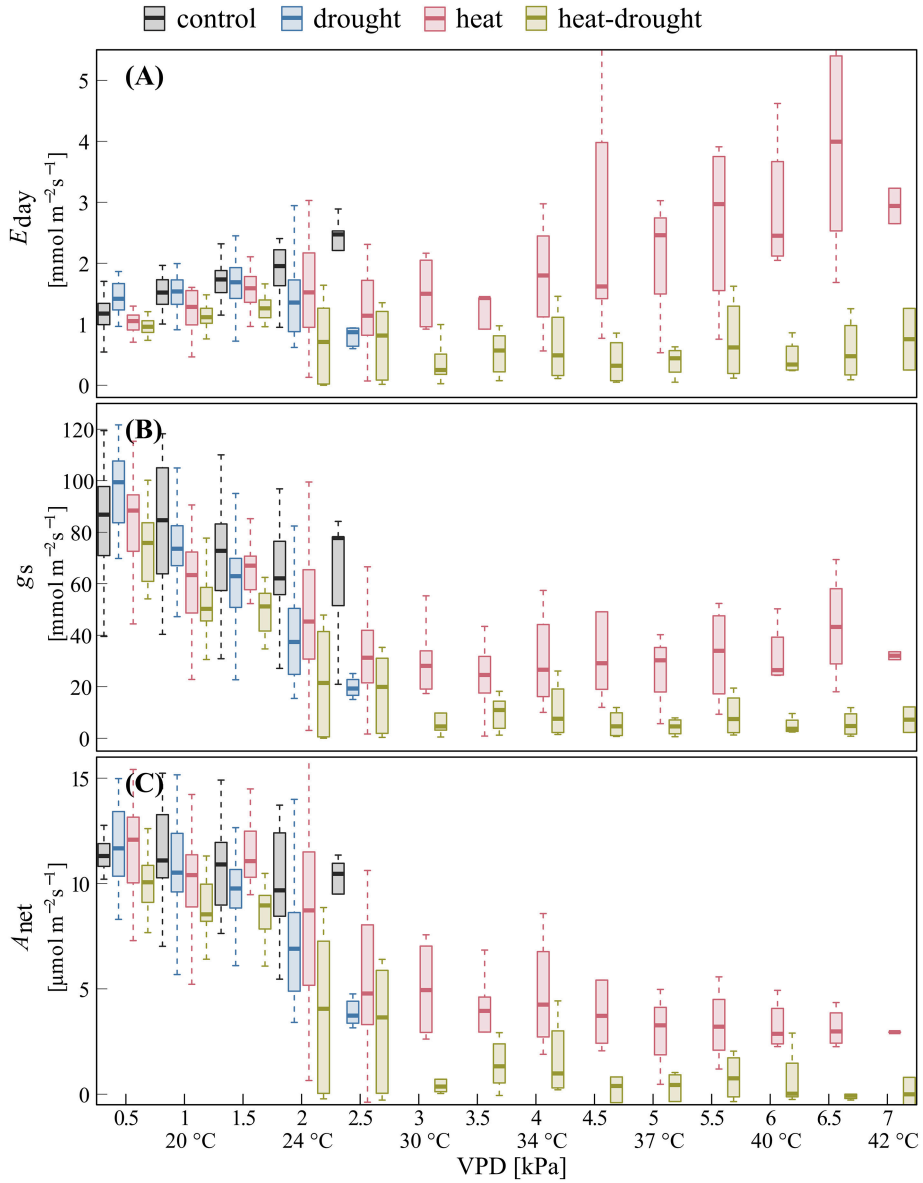

FIGURE 4 | Changes in shoot gas exchange in response to VPD for surviving trees. Given are day-time **(A)** transpiration E_{day}, **(B)** stomatal conductance g_s, and **(C)** net photosynthesis A_{net} in the control ($n = 4$), drought ($n = 4$), heat ($n = 3$), heat-drought ($n = 1$) treatment during before stress and heat wave conditions. Data are bin-averaged in VPD classes of 0.5 kPa (10 a.m.–7 p.m.).

with a treatment effect after recovery (ANOVA, $P \leq 0.001$). Dead seedlings showed accumulation of proline during both sampling campaigns. Proline content in roots was much smaller and no clear response to the treatments was found.

Shoot nitrate content, proposed here as an indirect measure for nitrogen (N) assimilation, was 2 to 4 times higher during stress in heat and heat-drought seedlings (*post-hoc*, $P \leq 0.05$) than the control or drought treatment. Following recovery, nitrate content in the heat treatment decreased to control levels, while it showed a lasting effect in the heat-drought treatment (ANOVA, $P \leq 0.05$) and remained elevated toward drought (*post-hoc*, $P \leq 0.05$). No obvious effect of the treatments on root nitrate was visible (**Figure 7D**). Again, the dead seedlings showed highest concentrations and no decline during recovery.

The osmotic potential (Π) of shoots remained relatively constant in all treatments throughout the experiment. Π in roots showed a tendency to decrease in the drought (treatment effect; ANOVA, $P \leq 0.05$) and heat-drought treatment although root total C declined (**Figure 6J**) because root water content was reduced (**Table S2**).

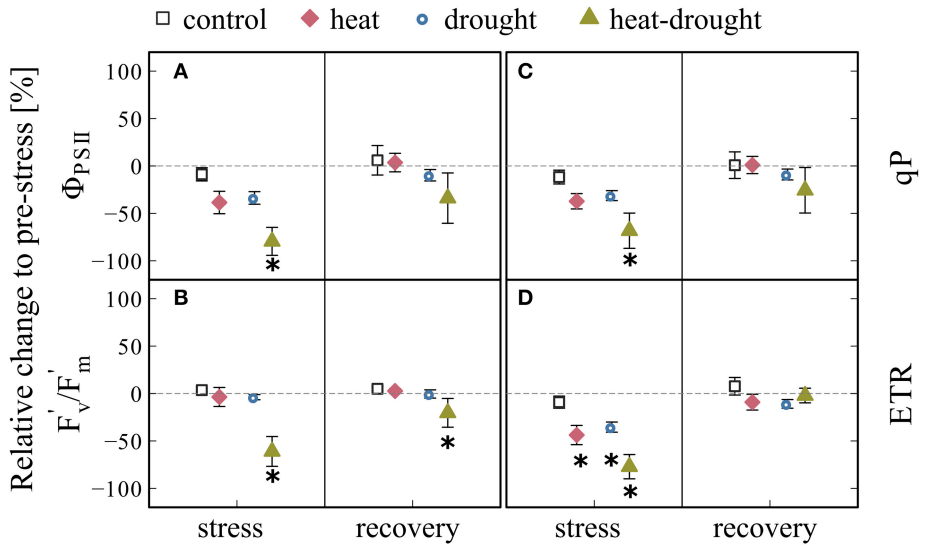

FIGURE 5 | Changes in chlorophyll fluorescence parameters during stress and recovery relative to before stress conditions. Parameters shown are: **(A)** effective photosystem II quantum yield (Φ_{PSII}), **(B)** maximum quantum yield of the photosystem II (F_v'/F_m'), **(C)** coefficients of photochemical fluorescence quenching (qP), **(D)** relative electron transfer rate (ETR). The error bars are ±1 SE ($n = 4$, but heat-drought treatment during recovery $n = 3$). The intermitted lines provide comparison to before stress conditions. Significant treatment effects are given *(ANOVA, $P \leq 0.05$).

DISCUSSION

High Temperature and Mortality

Although the exact cause of seedling mortality is not clear, it likely relates to the high shoot surface temperatures that developed in particular when transpiration ceased. As indicated by the high-resolution dendrometer data (**Figure S3**) seedlings in the heat-drought treatment died right after the last day of the first heat wave and desiccated rapidly afterwards. In contrast, seedlings in the heat treatment showed strong stem diameter declines, indicating death, only after the second heat wave had ended. Such a delay in stress response might indicate that cellular damage (e.g., in needles, roots and/or cambium cells) progresses over time, as has been observed after high temperature stress, e.g., Hüve et al. (2011), until critical levels are reached beyond which tree functioning cannot longer be maintained. This was also described as indirect damage by Colombo and Timmer (1992). The differences in the occurrence of mortality between heat and heat-drought treatments might reflect dosage effects of the experienced heat stress. The reduced transpiration in the heat-drought treatment (c. 0.5 mmol $m^{-2}s^{-1}$) vs. the heat treatment (c. 2 mmol $m^{-2}s^{-1}$) at a VPD of 4 kPa and 42°C air temperature resulted in 2.6°C higher needle temperatures at the end of the second heat wave (**Table 1**). Such an increase in leaf temperature has also been observed in mature forests when drought-exposed and well-watered trees were compared (Scherrer et al., 2011). With regard to the pronounced mortality under heat-drought as observed in our experiment, leaf cooling could have been crucial for survival as leaf temperatures had reached 47°C, a critical value for tissue damage in conifers (Colombo and Timmer, 1992; Bigras, 2000). The importance of evaporative cooling at lower VPD was examined recently for *Pinus taeda* (Urban et al., 2017b). The study showed that seedlings were able to keep stomata open to maintain high transpiration rates. This resulted in lower leaf temperatures. According to a field experiment on *Eucalyptus parramattensis* by Drake et al. (2018), leaf surface heating was reduced by 2.8°C on average because transpiration was maintained at high rates even at temperatures >43°C.

The ability of the pine seedlings to cool via transpiration was found to fail under the water limiting conditions applied here. Under field conditions, leaf cooling can be supported by transport of sensible heat via high wind speed or convective air flow. Such upward flow conditions and cooling of forest canopy have been shown at the Yatir forest (Rotenberg and Yakir, 2011; Eder et al., 2015). However, wind speed and convective exchange for small seedlings under canopy is lower as for mature trees. Also, tissue temperature is strongly affected by the closeness of bare and hot soil surfaces (Kolb and Robberecht, 1996). The authors found that under such conditions, seedlings with higher stomatal conductance were more likely to survive. This compares well to the findings that trees with low E_{day} and g_s died, while seedlings that maintained generally higher E_{day} rates survived (**Figure 2**). In summary, the high temperatures experienced by the seedlings in the heat and heat-drought treatment caused pronounced stress, likely resulting in membrane and protein damage causing higher mortality in trees with lower evaporative cooling capacity.

Stress Severity and Impairment of N Assimilation

The impact of heat and heat-drought stress was not only reflected in high mortality rates but also by highly elevated proline

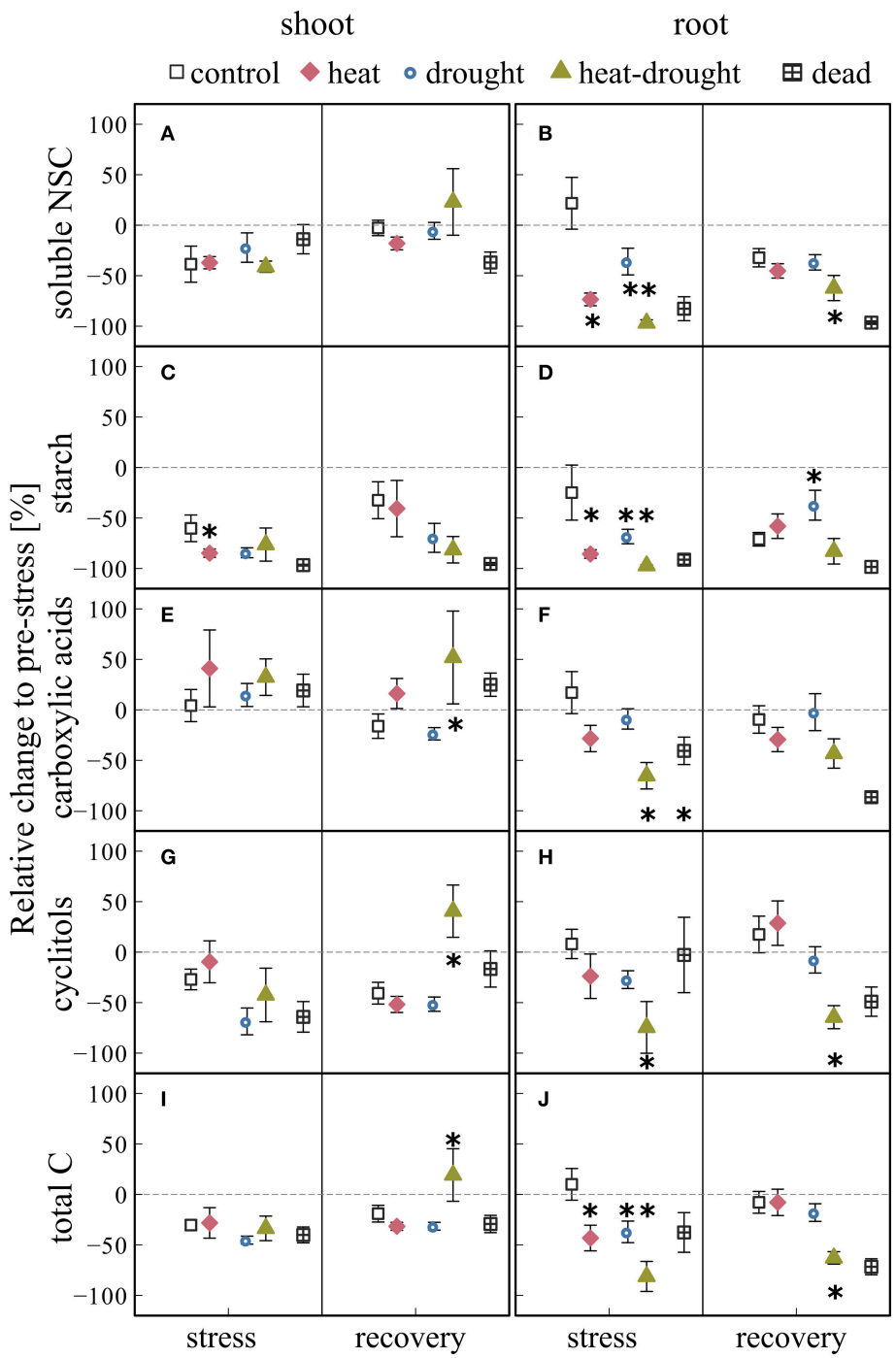

FIGURE 6 | Changes in non-structural carbohydrate (NSC) concentrations for shoot and root tissues during stress and recovery relative to before stress conditions. Shown are **(A,B)** soluble non-structural carbohydrates (soluble NSC: glucose, fructose, sucrose), **(C,D)** starch **(E,F)** carboxylic acids (malate, fumarate, citrate), **(G,H)** cyclitols (myo-inositol, D-pinitol), and **(I,J)** total carbohydrates (given as C6 equivalents of the shown metabolites) for control, drought, heat, heat-drought and dead seedlings. The error bars are ±1 SE ($n = 6$, but heat-drought during stress and recovery $n = 3$, dead heat samples $n = 5$, dead heat-drought samples $n = 15$). The intermitted lines provide comparison to before stress conditions. Significant treatment effects are given *(ANOVA, $P \leq 0.05$). See **Table S2** for absolute concentrations.

contents. Proline was not upregulated in response to the applied drought alone. However, drought stress can be viewed as rather mild, as stomata did not close completely and ψ_{shoot} remained well above critical values for xylem embolism formation (Oliveras et al., 2003; Delzon et al., 2010; Klein et al., 2011; David-Schwartz et al., 2016). Thus, function of proline as an osmoprotectant was of minor importance, which is in line with an unchanged Π of shoots during drought compared with control. It has been found

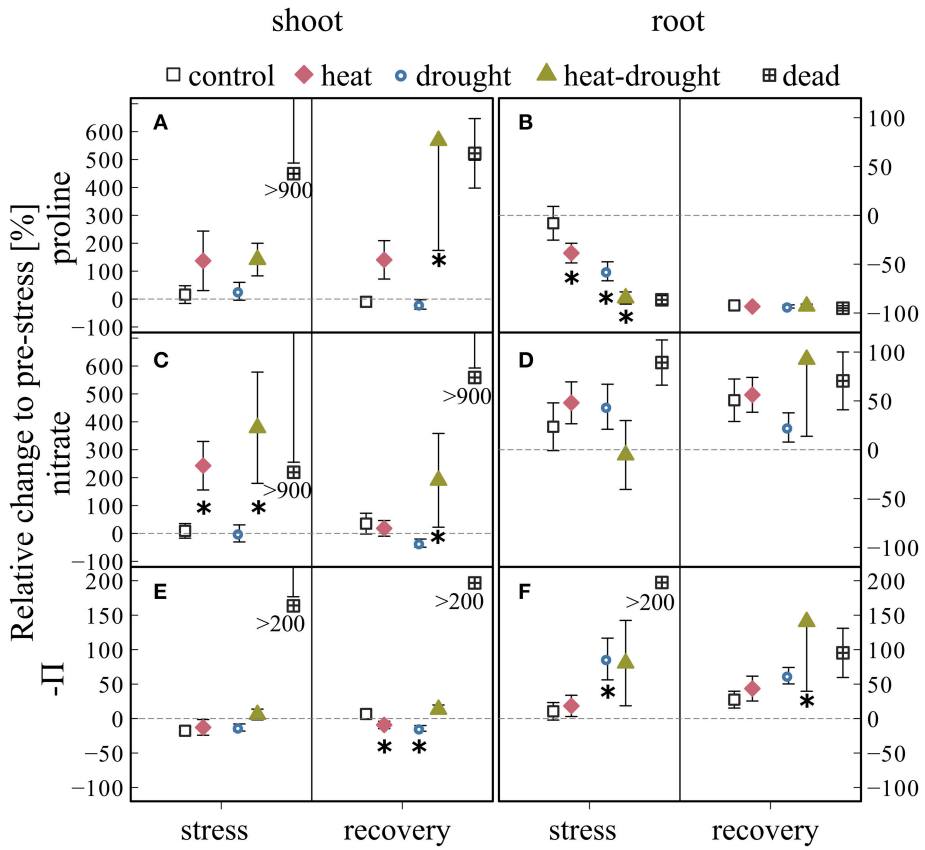

FIGURE 7 | Changes in **(A,B)** proline, **(C,D)** nitrate concentrations and osmotic potential Π **(E,F)** in shoots and roots during stress and recovery compared to before stress conditions for control, drought, heat, heat-drought and dead seedlings. Osmotic potential was calculated from measured solutes and tissue water content using the van't Hoff equation. The error bars are ±1 SE ($n = 6$, but heat-drought treatment during stress and recovery $n = 3$). The intermitted line provides comparison to before stress conditions. Significant treatment effects are given *(ANOVA, $P \leq 0.05$). In dead seedlings, when changes exceed axis scaling, the mean value was placed below the SE.

that proline accumulates under salinity stress (Hamilton, 2001; Hayat et al., 2012). Although not directly relevant it is interesting to note that a quadratic relationship between shoot chloride content and proline concentrations was found (**Figure S4**). This might have been caused by increased uptake of chloride by roots at high temperatures (Turner and Lahav, 1985).

Proline upregulation under heat stress is reported as beneficial for plants due to its role as protein stabilizer (e.g., complex II of mitochondrial electron transport chain; Hamilton, 2001). Moreover, proline synthesis serves as an efficient NADPH scavenger to regenerate $NADP^+$ (Szabados and Savouré, 2010; Hayat et al., 2012; Zhang et al., 2015) and to prevent radical production in the thylakoid electron transfer chain (Kramer et al., 2004). This mechanism might enhance ETR by regenerating electron acceptors, and thus reducing oxidative stress. Indeed, we found that ETR was unaffected in the heat treatment, while it was strongly reduced in the heat-drought treatment. Thus, the membrane and protein stabilizing ability of proline could not prevent photo-inhibition at the time of highest needle temperatures in the heat-drought treatment (>47°C).

Levels of nitrate in shoots of heat and heat-drought stressed Aleppo pines were elevated, while they did not change in roots, thus indicating heat-induced inactivation of leaf nitrogen assimilation. Decreased nitrate reductase activity has been observed to occur at temperatures above 40°C in cereals (Onwueme et al., 1971; Pal et al., 1976) and nitrate reductase activity recovers quickly after heat release. A fast recovery of N assimilation in Aleppo pine 2 days after stress release may also be concluded from the drop in leaf nitrate content (see **Figure 7**), while in the dead seedlings nitrate levels remained highly elevated (>900%).

Metabolic Responses Toward Heat-Drought Stress

The degree of stress and reduction in gas exchange were reflected in root NSC concentrations. In the heat-drought treatment, soluble NSC, starch, carboxylic acids and cyclitols declined to a larger extend than in the heat treatment although root zone temperatures were similar in both treatments (data not shown). Supposedly, the smaller C uptake in the heat-drought treatment decreased phloem transport (Ruehr et al.,

2009; Sevanto, 2014, 2018), which caused a strong depletion of soluble sugars and starch storage in roots. Total NSC levels were close to zero in the roots of the heat-drought seedlings, which may indicate critical C shortage in roots, limiting the otherwise high maintenance respiration in roots at high temperatures (Jarvi and Burton, 2018; Tjoelker, 2018). This could have affected root functionality and hence contributed to the observed large mortality rates in the heat-drought treatment.

Changes in lipids, which can be critical for C supply during stress, were not measured. In particular in pine trees, lipids (triglycerides) together with cyclitols are reported to be a large carbon storage pool (Piispanen and Saranpää, 2002; Hoch et al., 2003) and this pool can easily be channeled into the Tri-carboxylic-acid cycle especially during extreme stress (Fischer et al., 2015). This partly explains the weak responses of carboxylic acids under heat and heat-drought, whereas root NSC was depleted. Furthermore, carboxylic acids together with cyclitols, did surpass or at least equal the concentration of the typically measured NSC (starch, sucrose, glucose, and fructose; **Table S2**), and hence should be considered as important plant carbohydrate pools.

Carboxylic acids exert key functions in the regulatory network of plants. For example, intermediates from the tri-carboxylic-acid cycle (TCA) are important for the generation of ATP and thus key in respiratory processes. Additionally, they can provide carbon skeletons for amino acids and carbohydrates (Fernie et al., 2004). An increase in carboxylic acids during recovery might indicate enhanced investment into provision of carbon skeletons for maintenance and repair mechanisms. For heat-drought treated seedlings the accumulation of carboxylic acids can be explained by the reduction of R_{dark}. A similar upregulation of TCA intermediates was recently reported for eucalypts in response to heat and drought (Correia et al., 2018).

While shoot soluble NSC did not decline, shoot R_{dark} was much lower during the second than in the first heat wave and during the period of recovery. Presumably, available C for respiration was not limited in the heat-drought treatment at this stage because of actively maintained high sugar levels. This can be concluded from the upregulation of compatible solutes, including cyclitols during recovery. A similar pattern has also been observed in Scots pine where newly assimilated carbohydrates were allocated to cyclitols during recovery from drought (Galiano et al., 2017). Only heat-drought was associated with an increase in cyclitols during recovery, which might be explained by the very high needle temperatures that were found in this treatment and the protective function of cyclitols against heat denaturation (Jaindl and Popp, 2006).

Reports on NSC concentrations during drought have often been found to be inconclusive and to differ between species. Although hydraulic failure is often lethal, drought-induced lethality is not always connected to NSC depletion (Adams et al., 2017). In fact, NSC concentrations during drought were found to increase, decrease or remain constant in a wide range of tree species (Hartmann and Trumbore, 2016). Information on isolated heat effects on NSC of tree seedlings is scarce and might depend on heat dosage rather than temperature maxima. For example, it has been postulated that high temperatures lead to an increase in shoot NSC (Sevanto and Dickman, 2015). Also, Marias et al. (2017) have found an increase of sugars in shoots, when coffee plants have been exposed to a heat pulse (49°C for 45 min). This is in stark contrast to our observations of relatively unchanged NSC levels in shoots and declining NSC in roots during the heat and heat-drought treatment. We suggest that the key for explaining the results is the duration of the experiment, which is corroborated by findings that longer stress periods did also not change NSC concentrations in leaves of *Eucalyptus globulus,* while NSC concentrations declined when treated with additional drought (Correia et al., 2018). To conclude this section, the primary metabolism of Aleppo pine shoots appears to be highly buffered against deviations even under extraordinary stressful conditions. In contrast, the root metabolism decouples from the source supply under mild drought and/or extreme heat waves and is clearly affected by combined stressors. These changes in allocation patterns might indicate an approach to preserve source functionality at the cost of sink integrity.

Photosynthetic Inhibition and Recovery From Acute Heat Stress

Water availability during heat waves seems to be a key factor of survival (Bauweraerts et al., 2014; Ruehr et al., 2016) since it translates in evaporative cooling capacity (Drake et al., 2018) and protects the photosynthetic apparatus. This is supported by leaf fluorescence that showed only a moderate decline under heat stress (only ETR; *post-hoc*, $P \leq 0.05$) while in heat-drought trees chlorophyll fluorescence parameters (ΦPSII, F'_v/F'_m, qP, and ETR) decreased strongly. A decline in ΦPSII indicates a saturation of the electron transfer chain, bearing the risk of oxidative stress (Murchie and Lawson, 2013). A reduction of ΦPSII due to pigment degeneration can be neglected because of their stability above 60°C (Rätsep et al., 2018) and only temperatures above 50°C are considered critical for the disaggregation of the harvesting complexes (Tang et al., 2007; Nellaepalli et al., 2014). ETR, on the other hand, largely depends on thylakoid membrane integrity, which is disturbed at much lower temperatures of about 38°C (Havaux et al., 1996; Bukhov et al., 1999). Dark-adapted maximum operating efficiency F_v/F_m is widely used for the estimation of stress severity (Murchie and Lawson, 2013). In this experiment, F'_v/F'_m (light-adapted) was recorded instead. This parameter decreases with increasing non-photochemical quenching (Murchie and Lawson, 2013), which means the dissipation of excess energy by heat. Together with the hypothesis of a saturated photosystem and reduced ETR, this provides evidence for stress-induced limitations of processes downstream of the light reaction of photosynthesis. There is increasing evidence that thresholds for irreparable/slowly recoverable damage are typically reached at temperatures >45°C in temperate regions (Hüve et al., 2011).

The apparent small decline of chlorophyll fluorescence parameters in the heat treatment, measured 1 day after the last heat wave had ended, may either reflect a relative mild impairment of the photosynthetic apparatus, or indicate a fast recovery of chlorophyll fluorescence parameters 1 day after the acute stress. Fast recovery responses of photosynthetic parameters after acute heat waves (when water was not limiting) were observed in herbaceous plants, as well as in some tree species and typically relate to temperatures <45°C (Hüve et al., 2011; Ameye et al., 2012; Guha et al., 2018). However, complete recovery of the few surviving seedlings in the heat-drought treatment seemed to be impaired.

Canopy Gas Exchange Affected by High Temperatures, Atmospheric Demand and Soil Drought

Heat stress, which induces high atmospheric evaporative demand has been reported to result in (partial) stomatal closure (Ameye et al., 2012; Bauweraerts et al., 2013; Duarte et al., 2016; Garcia-Forner et al., 2016; Ruehr et al., 2016). In our study, we found that stomata did not fully close in the heat treatment even under extreme vapor pressure deficits of >6 kPa. Indeed, partial stomatal closure was enough to maintain midday stem WP at moderate levels of −1.2 MPa (measured at the last day of the second heat wave), indicating that the xylem water transport was operating under non-harmful conditions. Under the same atmospheric conditions but reduced irrigation, the stress on the hydraulic system of the seedlings was larger (−1.8 MPa) and stomata were almost fully closed preventing any further drop in ψ_{shoot} and hence xylem embolism. Separating the effects of high temperature and VPD on stomatal responses is challenging. In experiments with temperature rise independent of VPD, g_s has been shown to increase (Urban et al., 2017a,b). A temperature-driven increase in g_s might simply reflect enhanced water loss along with rising temperatures without any further opening of stomata aperture, or could reflect an active cooling mechanism that prevents further closing of stomata. While the mechanism has not yet been explained in detail, various results indicate an active role of leaf cooling as a reasonable option (Urban et al., 2017a,b; Drake et al., 2018).

A_{net} and E_{day} were uncoupled during the heat waves, resulting in a strong decline in WUE_a. Both, fluxes showed slightly different response pattern during the first and the second heat wave with a less pronounced decrease in A_{net} in the former and a less pronounced increase in E_{day} during the latter. This resulted in similar amplitudes of WUE_a decrease in both heat waves. R_{dark} was similarly dampened during the second heat wave, especially in the surviving heat-drought seedling. A similar decline in the amplitudes of gas exchange in response to repeated heat waves had been reported before for various other tree species (Duarte et al., 2016; Guha et al., 2018) and had been linked to cellular damage. Also WUE_i remained elevated during recovery from combined heat and drought stress. This was at the cost of reduced transpiration, which resulted in higher needle surface temperatures along with elevated levels of compatible solutes and dramatically changed shoot-to-root C allocation patterns.

CONCLUSION

The combination of heat and drought stress affected Aleppo pine seedlings differently than drought or heat alone. This was not restricted to the stress periods *per se*, but became more pronounced during post-stress since high mortality rates and delayed recovery of the surviving seedlings occurred. The observed delay in recovery and pronounced mortality in the heat-drought treatment clearly demonstrated that physiological stress responses can continue after environmental stress has been released. Moreover, it showed that a tight regulation of a plant's water balance via stomatal closure at the cost of evaporative cooling can result in excessive needle temperatures under the experimental conditions applied here. Although the exact cause of seedling death is difficult to depict, it is likely that observed needle temperatures (>47°C) either directly damaged shoot tissues or indirectly affected root vitality via reduced C translocation. In summary, we conclude that increases in heat wave temperatures, as predicted to occur during the next decades, can have disastrous effects in dry environments. It seems that in semi-arid forests where drought is a common phenomenon, even a single heat wave that surpasses a given threshold (probably above 47°C needle temperature) may have widely detrimental effects.

DATA AVAILABILITY STATEMENT

All relevant data is contained within the manuscript and the supplementary files. Shoot gas exchange data will be made available by the authors upon request.

AUTHOR CONTRIBUTIONS

AA, BB, NR, and RG designed the study. BB, MG, and NR conducted experiments. AH, BB, and MG conducted measurements. AH, BB, and NR contributed to data evaluation. BB and NR wrote the manuscript. AA, AH, MG, and RG contributed to revision.

FUNDING

This work was supported, in part, by the German Research Foundation through its German-Israeli project cooperation program Climate feedbacks and benefits of semi-arid forests (CliFF; grant no. YA 274/1-1 and SCHM 2736/2-1) and by the German Federal Ministry of Education and Research (BMBF), through the Helmholtz Association and its research program ATMO. NR acknowledges support by the German Research Foundation through its Emmy Noether Program (RU 1657/2-1). BB acknowledges support by GRACE–graduate school for climate and environment financed through the Helmholtz Association. We acknowledge support by Deutsche Forschungsgemeinschaft

and Open Access Publishing Fund of Karlsruhe Institute of Technology.

ACKNOWLEDGMENTS

The authors would like to thank Andreas Gast for technical support, Ines Bamberger, Sina Rogozinski, and Lena Mueller for their help during the experiment, and Simon Stutz, Lisa Wolf, and Imke Hörmiller for lab assistance. We want to thank Dan Yakir, Yakir Preisler, and Fedor Tatarinov for meteorological data and fruitful discussions.

SUPPLEMENTARY MATERIAL

The Supplementary Material for this article can be found online at: https://www.frontiersin.org/articles/10.3389/ffgc.2018.00008/full#supplementary-material

REFERENCES

Adams, H. D., Zeppel, M. J. B., Anderegg, W. R. L., Hartmann H., Landhäusser S. M., Tissue D. T., et al. (2017). A multi-species synthesis of physiological mechanisms in drought-induced tree mortality. *Nat. Ecol. Evol.* 1, 1285–1291. doi: 10.1038/s41559-017-0248-x

Allen, C. D., Breshears, D. D., and McDowell, N. G. (2015). On underestimation of global vulnerability to tree mortality and forest die-off from hotter drought in the Anthropocene. *Ecosphere* 6:art129. doi: 10.1890/ES15-00203.1

Allen, C. D., Macalady, A. K., Chenchouni, H., Bachelet, D., McDowell, N., Vennetier M., et al. (2010). A global overview of drought and heat-induced tree mortality reveals emerging climate change risks for forests. *Forest Ecol. Manage.* 259, 660–684. doi: 10.1016/j.foreco.2009.09.001

Ameye, M., Wertin, T. M., Bauweraerts, I., McGuire, M. A., Teskey, R. O., Steppe K., et al. (2012). The effect of induced heat waves on *Pinus taeda* and *Quercus rubra* seedlings in ambient and elevated CO_2 atmospheres. *N. Phytol.* 196, 448–461. doi: 10.1111/j.1469-8137.2012.04267.x

Anderegg, W. R., Hicke, J. A., Fisher, R. A., Allen, C. D., Aukema, J., Bentz, B., et al. (2015). Tree mortality from drought, insects, and their interactions in a changing climate. *N. Phytol.* 208, 674–683. doi: 10.1111/nph.13477

Anderegg, W. R. L., Kane, J. M., and Anderegg, L. D. L. (2012). Consequences of widespread tree mortality triggered by drought and temperature stress. *Nat. Clim. Change* 3, 30–36. doi: 10.1038/nclimate1635

Anderegg, W. R. L., Wolf, A., Arango-Velez, A., Choat, B., Chmura, D. J., Jansen, S., et al. (2018). Woody plants optimise stomatal behaviour relative to hydraulic risk. *Ecol. Lett.* 21, 968–977. doi: 10.1111/ele.12962

Bamberger, I., Ruehr, N. K., Schmitt, M., Gast, A., Wohlfahrt, G., Arneth, A., et al. (2017). Isoprene emission and photosynthesis during heatwaves and drought in black locust. *Biogeosciences* 14, 3649–3667. doi: 10.5194/bg-14-3649-2017

Bates, D., Machler, M., Bolker, B., and Walker, S. (2015). Fitting linear mixed-effects models using lme4. *J. Stat. Softw.* 67, 1–48. doi: 10.18637/jss.v067.i01

Bauweraerts, I., Ameye, M., Wertin, T. M., McGuire, M. A., Teskey, R. O., Steppe, K., et al. (2014). Water availability is the decisive factor for the growth of two tree species in the occurrence of consecutive heat waves. *Agricul. Forest Meteorol.* 189–190, 19–29. doi: 10.1016/j.agrformet.2014.01.001

Bauweraerts, I., Wertin, T. M., Ameye, M., McGuire, MA, Teskey, R. O., and Steppe K. (2013). The effect of heat waves, elevated [CO_2] and low soil water availability on northern red oak (*Quercus rubra* L.) seedlings. *Glob. Change Biol.* 19, 517–528. doi: 10.1111/gcb.12044

Bigras, F. J. (2000). Selection of white spruce families in the context of climate change: heat tolerance. *Tree Physiol.* 20, 1227–1234. doi: 10.1093/treephys/20.18.1227

Blessing, C. H., Werner, R. A., Siegwolf, R., and Buchmann N. (2015). Allocation dynamics of recently fixed carbon in beech saplings in response to increased temperatures and drought. *Tree Physiol.* 35, 585–598. doi: 10.1093/treephys/tpv024

Bonan, G. B., Williams, M., Fisher, R. A., and Oleson, K. W. (2014). Modeling stomatal conductance in the earth system: linking leaf water-use efficiency and water transport along the soil–plant–atmosphere continuum. *Geosci. Model Dev.* 7, 2193–2222. doi: 10.5194/gmd-7-2193-2014

Brauner, K., Hörmiller, I., Nägele, T., and Heyer, A. G. (2014). Exaggerated root respiration accounts for growth retardation in a starchless mutant of *Arabidopsis thaliana*. *Plant J.* 79, 82–91. doi: 10.1111/tpj.12555

Bukhov, N. G., Wiese, C., Neimanis, S., and Heber U. (1999). Heat sensitivity of chloroplasts and leaves: leakage of protons from thylakoids and reversible activation of cyclic electron transport. *Photosynth. Res.* 59, 81–93. doi: 10.1023/A:1006149317411

Burghardt, M., and Riederer, M. (2003). Ecophysiological relevance of cuticular transpiration of deciduous and evergreen plants in relation to stomatal closure and leaf water potential. *J. Exp. Bot.* 54, 1941–1949. doi: 10.1093/jxb/erg195

Colombo, S. J., and Timmer, V. R. (1992). Limits of tolerance to high temperatures causing direct and indirect damage to black spruce. *Tree Physiol.* 11, 95–104. doi: 10.1093/treephys/11.1.95

Correia, B., Hancock, R. D., Amaral, J., Gomez-Cadenas, A., Valledor, L., and Pinto, G. (2018). Combined drought and heat activates protective responses in *Eucalyptus globulus* that are not activated when subjected to drought or heat stress alone. *Front. Plant Sci.* 9:233. doi: 10.3389/fpls.2018.00819

David-Schwartz, R., Paudel, I., Mizrachi, M., Delzon, S., Cochard, H., Lukyanov, V., et al. (2016). Indirect evidence for genetic differentiation in vulnerability to embolism in *Pinus halepensis*. *Front. Plant Sci.* 7:768. doi: 10.3389/fpls.2016.00768

Delzon, S., Douthe, C., Sala, A., and Cochard, H. (2010). Mechanism of water-stress induced cavitation in conifers: bordered pit structure and function support the hypothesis of seal capillary-seeding. *Plant Cell Environ.* 33, 2101–2111. doi: 10.1111/j.1365-3040.2010.02208.x

Drake, J. E., Tjoelker, M. G., Vårhammar, A., Medlyn, B. E., Reich, P. B., Leigh, A., et al. (2018). Trees tolerate an extreme heatwave via sustained transpirational cooling and increased leaf thermal tolerance. *Glob. Change Biol.* 24, 2390–2402. doi: 10.1111/gcb.14037

Duarte, A. G., Katata, G., Hoshika, Y., Hossain, M., Kreuzwieser, J., Arneth, A., et al. (2016). Immediate and potential long-term effects of consecutive heat waves on the photosynthetic performance and water balance in Douglas-fir. *J. Plant Physiol.* 205, 57–66. doi: 10.1016/j.jplph.2016.08.012

Eder, F., Roo, F., de, Rotenberg, E., Yakir, D., Schmid, H. P., Mauder, M., et al. (2015). Secondary circulations at a solitary forest surrounded by semi-arid shrubland and their impact on eddy-covariance measurements. *Agricul. Forest Meteorol.* 211–212, 115–127. doi: 10.1016/j.agrformet.2015.06.001

Fernie, A. R., Carrari, F., and Sweetlove, L. J. (2004). Respiratory metabolism: glycolysis, the TCA cycle and mitochondrial electron transport. *Curr. Opin. Plant Biol.* 7, 254–261. doi: 10.1016/j.pbi.2004.03.007

Fischer, S., Hanf, S., Frosch, T., Gleixner, G., Popp, J., Trumbore, S., et al. (2015). *Pinus sylvestris* switches respiration substrates under shading but not during drought. *N. Phytol.* 207, 542–550. doi: 10.1111/nph.13452

Galiano, L., Timofeeva, G., Saurer, M., Walter Siegwolf, R. T., Martínez-Vilalta, J., Hommel, R., et al. (2017). The fate of recently fixed carbon after drought release: towards unravelling C storage regulation in *Tilia platyphyllos* and *Pinus sylvestris*. *Plant Cell Environ.* 40, 1711–1724. doi: 10.1111/pce.12972

Garcia-Forner, N., Adams, H. D., Sevanto, S., Collins, A.D., Dickman, L. T., Hudson, P. J., et al. (2016). Responses of two semiarid conifer tree species to reduced precipitation and warming reveal new perspectives for stomatal regulation. *Plant Cell Environ.* 39, 38–49. doi: 10.1111/pce.12588

Giorgi, F., and Lionello, P. (2008). Climate change projections for the Mediterranean region. *Glob. Planetary Change* 63, 90–104. doi: 10.1016/j.gloplacha.2007.09.005

Guha, A., Han, J., Cummings, C., McLennan, D., and Warren, J. W. (2018). Differential ecophysiological responses and resilience to heat wave events in four co-occurring temperate tree species. *Environ. Res. Lett.* 13:65008. doi: 10.1088/1748-9326/aabcd8

Haldimann, P., and Feller, U. (2004). Inhibition of photosynthesis by high temperature in oak (*Quercus pubescens* L.) leaves grown under natural conditions closely correlates with a reversible heat-dependent reduction of the activation state of ribulose-1,5-bisphosphate carboxylase/oxygenase. *Plant Cell Environ.* 27, 1169–1183. doi: 10.1111/j.1365-3040.2004.01222.x

Hamilton, E. W. (2001). Mitochondrial adaptations to NaCl. Complex I is protected by anti-oxidants and small heat shock proteins, whereas complex II is protected by proline and betaine. *Plant Physiol.* 126, 1266–1274. doi: 10.1104/pp.126.3.1266

Hartmann, H., and Trumbore, S. (2016). Understanding the roles of nonstructural carbohydrates in forest trees–from what we can measure to what we want to know. *N. Phytol.* 211, 386–403. doi: 10.1111/nph.13955

Havaux, M., Tardy, F., Ravenel, J., Chanu, D., and Parot, P. (1996). Thylakoid membrane stability to heat stress studied by flash spectroscopic measurements of the electrochromic shift in intact potato leaves: influence of the xanthophyll content. *Plant Cell Environ.* 19, 1359–1368. doi: 10.1111/j.1365-3040.1996.tb00014.x

Hayat, S., Hayat, Q., Alyemeni, M. N., Wani, A. S., Pichtel, J., and Ahmad A. (2012). Role of proline under changing environments: a review. *Plant Signal. Behav.* 7, 1456–1466. doi: 10.4161/psb.21949

Hays, L. M., Crowe, J. H., Wolkers, W., and Rudenko S. (2001). Factors affecting leakage of trapped solutes from phospholipid vesicles during thermotropic phase transitions. *Cryobiology* 42, 88–102. doi: 10.1006/cryo.2001.2307

Hoch, G., Richter, A., and Körner, C. (2003). Non-structural carbon compounds in temperate forest trees. *Plant Cell Environ.* 26, 1067–1081. doi: 10.1046/j.0016-8025.2003.01032.x

Hüve, K., Bichele, I., Rasulov, B., and Niinemets U. (2011). When it is too hot for photosynthesis: heat-induced instability of photosynthesis in relation to respiratory burst, cell permeability changes and H2O2 formation. *Plant Cell Environ.* 34, 113–126. doi: 10.1111/j.1365-3040.2010.02229.x

Jaindl, M., and Popp, M. (2006). Cyclitols protect glutamine synthetase and malate dehydrogenase against heat induced deactivation and thermal denaturation. *Biochem. Biophys. Res. Commun.* 345, 761–765. doi: 10.1016/j.bbrc.2006.04.144

Jarvi, M. P., and Burton, A. J. (2018). Adenylate control contributes to thermal acclimation of sugar maple fine-root respiration in experimentally warmed soil. *Plant Cell Environ.* 41, 504–516. doi: 10.1111/pce.13098

Jarvis, P. G. (1976). The interpretation of the variations in leaf water potential and stomatal conductance found in canopies in the field. *Philos. Transac. R. Soc. B Biol. Sci.* 273, 593–610. doi: 10.1098/rstb.1976.0035

Klein, T., Cohen, S., and Yakir, D. (2011). Hydraulic adjustments underlying drought resistance of *Pinus halepensis*. *Tree Physiol.* 31, 637–648. doi: 10.1093/treephys/tpr047

Klein, T., and Niu, S. (2014). The variability of stomatal sensitivity to leaf water potential across tree species indicates a continuum between isohydric and anisohydric behaviours. *Funct. Ecol.* 28, 1313–1320. doi: 10.1111/1365-2435.12289

Kolb, P. F., and Robberecht, R. (1996). High temperature and drought stress effects on survival of Pinus ponderosa seedlings. *Tree Physiol.* 16, 665–672. doi: 10.1093/treephys/16.8.665

Kramer, D. M., Avenson, T. J., and Edwards, G. E. (2004). Dynamic flexibility in the light reactions of photosynthesis governed by both electron and proton transfer reactions. *Trends Plant Sci.* 9, 349–357. doi: 10.1016/j.tplants.2004.05.001

Liu, H., Williams, P. A., Allen, C. D., Guo, D., Wu, X., Anenkhonov, O. A., et al. (2013). Rapid warming accelerates tree growth decline in semi-arid forests of Inner Asia. *Glob. Change Biol.* 19, 2500–2510. doi: 10.1111/gcb.12217

Marias, D. E., Meinzer, F. C., and Still, C. (2017). Impacts of leaf age and heat stress duration on photosynthetic gas exchange and foliar nonstructural carbohydrates in Coffea arabica. *Ecol. Evol.* 7, 1297–1310. doi: 10.1002/ece3.2681

Meehl, G. A., and Tebaldi, C. (2004). More intense, more frequent, and longer lasting heat waves in the 21st century. *Science* 305, 994–997. doi: 10.1126/science.1098704

Monod, B., Collin, A., Parent, G., and Boulet P. (2009). Infrared radiative properties of vegetation involved in forest fires. *Fire Safety J.* 44, 88–95. doi: 10.1016/j.firesaf.2008.03.009

Murchie, E. H., and Lawson, T. (2013). Chlorophyll fluorescence analysis: a guide to good practice and understanding some new applications. *J. Exp. Bot.* 64, 3983–3998. doi: 10.1093/jxb/ert208

Nellaepalli, S., Zsiros, O., Tóth, T., Yadavalli, V., Garab, G., Subramanyam, R., et al. (2014). Heat- and light-induced detachment of the light harvesting complex from isolated photosystem I supercomplexes. *J. Photochem. Photobiol. B Biol.* 137, 13–20. doi: 10.1016/j.jphotobiol.2014.04.026

Niinemets, Ü. (2018). When leaves go over the thermal edge. *Plant Cell Environ.* 41, 1247–1250. doi: 10.1111/pce.13184

Oliveras, I., Martínez-Vilalta, J., Jimenez-Ortiz, T., José Lledó, M., Escarré, A., and Piñol, J. (2003). Hydraulic properties of *Pinus halepensis*, Pinus pinea and *Tetraclinis articulata* in a dune ecosystem of Eastern Spain a dune ecosystem of Eastern Spain. *Plant Ecol.* 169, 131–141. doi: 10.1023/A:1026223516580

Onwueme, I. C., Laude, H. M., and Huffaker, R. C. (1971). Nitrate reductase activity in relation to heat stress in barley seedlings. *Crop Sci.* 11, 195–200. doi: 10.2135/cropsci1971.0011183X001100020009x

O'sullivan, O. S., Heskel, M. A., Reich, P. B., Tjoelker, M. G., Weerasinghe, L. K., Penillard, A., et al. (2017). Thermal limits of leaf metabolism across biomes. *Glob. Change Biol.* 23, 209–223. doi: 10.1111/gcb.13477

Pal, U. R., Johnson, R. R., and Hageman, R. H. (1976). Nitrate reductase activity in heat (drought) tolerant and intolerant maize genotypes. *Crop Sci.* 16, 775–779. doi: 10.2135/cropsci1976.0011183X001600060009x

Piispanen, R., and Saranpää, P. (2002). Neutral lipids and phospholipids in Scots pine (*Pinus sylvestris*) sapwood and heartwood. *Tree Physiol.* 22, 661–666. doi: 10.1093/treephys/22.9.661

Quentin, A. G., Pinkard, E. A., Ryan, M. G., Tissue, D. T., Baggett, L. S., Adams, H. D., et al. (2015). Non-structural carbohydrates in woody plants compared among laboratories. *Tree Physiol.* 35, 1146–1165. doi: 10.1093/treephys/tpv073

Quinn, P. J. (1988). Effects of temperature on cell membranes. *Symp. Soc. Exp. Biol.* 42, 237–258.

R Core Team (2015). *R: A Language and Environment for Statistical Computing*. Vienna: R Foundation for Statistical Computing. Available online at: https://www.R-project.org/

Rashid, M. A., Andersen, M. N., Wollenweber, B., Kørup, K., Zhang, X., and Olesen J. E. (2018). Impact of heat-wave at high and low vpd on photosynthetic components of wheat and their recovery. *Environ. Exp. Bot.* 147, 138–146. doi: 10.1016/j.envexpbot.2017.12.009

Rätsep, M., Muru, R., and Freiberg, A. (2018). High temperature limit of photosynthetic excitons. *Nat. Commun.* 9:99. doi: 10.1038/s41467-017-02544-7

Rienth, M., Romieu, C., Gregan, R., Walsh, C., Torregrosa, L., Kelly, M. T., et al. (2014). Validation and application of an improved method for the rapid determination of proline in grape berries. *J. Agric. Food Chem.* 62, 3384–3389. doi: 10.1021/jf404627n

Ripullone, F., Guerrieri, M. R., Nole, A., Magnani, F., and Borghetti, M. (2007). Stomatal conductance and leaf water potential responses to hydraulic conductance variation in Pinus pinaster seedlings. *Trees* 21, 371–378. doi: 10.1007/s00468-007-0130-6

Rotenberg, E., and Yakir, D. (2010). Contribution of semi-arid forests to the climate system. *Science* 327, 451–454. doi: 10.1126/science.1179998

Rotenberg, E., and Yakir, D. (2011). Distinct patterns of changes in surface energy budget associated with forestation in the semiarid region. *Glob. Change Biol/.* 17, 1536–1548. doi: 10.1111/j.1365-2486.2010.02320.x

Ruehr, N. K., Gast, A., Weber, C., Daub, B., Arneth, A. (2016). Water availability as dominant control of heat stress responses in two contrasting tree species. *Tree Physiol.* 36, 164–178. doi: 10.1093/treephys/tpv102

Ruehr, N. K., Offermann, C. A., Gessler, A., Winkler JB, Ferrio JP, Buchmann N, et al. (2009). Drought effects on allocation of recent carbon: from beech leaves to soil CO2 efflux. *N. Phytol.* 184, 950–961. doi: 10.1111/j.1469-8137.2009.03044.x

Schär, C. (2015). Climate extremes: the worst heat waves to come. *Nat. Climate Change* 6, 128–129. doi: 10.1038/nclimate2864

Scherrer, D., Bader, M. K. F., and Körner, C. (2011). Drought-sensitivity ranking of deciduous tree species based on thermal imaging of forest canopies. *Agricul. Forest Meteorol.* 151, 1632–1640. doi: 10.1016/j.agrformet.2011.06.019

Seneviratne, S. I., Nicholls, N., Easterling, D., Goodess, C. M., Kanae, S., Kossin, J., et al. (2012). "Changes in climate extremes and their impacts on the natural physical environment" in *Managing the Risks of Extreme Events and Disasters to Advance Climate Change Adaptation. A Special Report of Working Groups I and II of the Intergovernmental Panel on Climate Change (IPCC)*, eds C. B. Field, V. Barros, T. F. Stocker, D. Qin, D. J. Dokken, K. L. Ebi, M. D. Mastrandrea, K. J. Mach, K. Plattner, S. K. Allen, M. Tignor, and P. M. Midgley (Cambridge, UK; New York, NY: Cambridge University Press), 109–230.

Sevanto, S. (2014). Phloem transport and drought. *J. Exp. Bot.* 65, 1751–1759. doi: 10.1093/jxb/ert467

Sevanto, S. (2018). Drought impacts on phloem transport. *Curr. Opin. Plant Biol.* 43, 76–81. doi: 10.1016/j.pbi.2018.01.002

Sevanto, S., and Dickman, L. T. (2015). Where does the carbon go?–Plant carbon allocation under climate change. *Tree Physiol.* 35, 581–584. doi: 10.1093/treephys/tpv059

Szabados, L., and Savouré, A. (2010). Proline: a multifunctional amino acid. *Trends Plant Sci.* 15, 89–97. doi: 10.1016/j.tplants.2009.11.009

Tabari, H., and Willems, P. (2018). Seasonally varying footprint of climate change on precipitation in the Middle East. *Sci. Rep.* 8:4435. doi: 10.1038/s41598-018-22795-8

Tang, Y., Wen, X., Lu, Q., Yang, Z., Cheng, Z., Lu, C., et al. (2007). Heat stress induces an aggregation of the light-harvesting complex of photosystem II in spinach plants. *Plant Physiol.* 143, 629–638. doi: 10.1104/pp.106.090712

Tatarinov, F., Rotenberg, E., Maseyk, K., Ogée, J., Klein, T., Yakir, D., et al. (2015). Resilience to seasonal heat wave episodes in a Mediterranean Pine Forest. *N. Phytol.* 210, 485–496, doi: 10.1111/nph.13791

Teskey, R., Wertin, T., Bauweraerts, I., Ameye, M., McGuire, M. A., Steppe, K., et al. (2015). Responses of tree species to heat waves and extreme heat events. *Plant Cell Environ.* 38, 1699–1712. doi: 10.1111/pce.12417

Tjoelker, M. G. (2018). The role of thermal acclimation of plant respiration under climate warming: putting the brakes on a runaway train? *Plant Cell Environ.* 41, 501–503. doi: 10.1111/pce.13126

Turner, D. W., and Lahav, E. (1985). Temperature influences nutrient absorption and uptake rates of bananas grown in controlled environments. *Scientia Horticul.* 26, 311–322. doi: 10.1016/0304-4238(85)90015-9

Urban, J., Ingwers, M., McGuire, M. A., and Teskey, R. O. (2017a). Stomatal conductance increases with rising temperature. *Plant Signal. Behav.* 12:e1356534. doi: 10.1080/15592324.2017.1356534

Urban, J., Ingwers, M. W., McGuire, M. A., and Teskey, R. O. (2017b). Increase in leaf temperature opens stomata and decouples net photosynthesis from stomatal conductance in pinus taeda and populus deltoides x nigra. *J. Exp. Bot.* 68, 1757–1767. doi: 10.1093/jxb/erx052

Verbruggen, N., and Hermans, C. (2008). Proline accumulation in plants: a review. *Amino Acids* 35, 753–759. doi: 10.1007/s00726-008-0061-6

Watson, H. (2015). Biological membranes. *Essays Biochem.* 59, 43–69. doi: 10.1042/bse0590043

Wieser, G., Oberhuber, W., Waldboth, B., Gruber, A., Matyssek, R., Siegwolf, R. T. W., et al. (2018). Long-term trends in leaf level gas exchange mirror tree-ring derived intrinsic water-use efficiency of Pinus cembra at treeline during the last century. *Agricul. Forest Meteorol.* 248, 251–258. doi: 10.1016/j.agrformet.2017.09.023

Williams, P. A., Allen, C. D., Macalady, A. K., Griffin, D., Woodhouse, C. A., Meko, D. M., et al. (2012). Temperature as a potent driver of regional forest drought stress and tree mortality. *Nat. Climate Change* 3, 292–297. doi: 10.1038/nclimate1693

Zang, U., Goisser, M., Häberle, K. H., Matyssek, R., Matzner, E., and Borken, W. (2014). Effects of drought stress on photosynthesis, rhizosphere respiration, and fine-root characteristics of beech saplings: a rhizotron field study. *Z. Pflanzenernähr. Bodenk.* 177, 168–177. doi: 10.1002/jpln.201300196

Zhang, L., Alfano, J. R., and Becker, D. F. (2015). Proline metabolism increases katG expression and oxidative stress resistance in *Escherichia coli*. *J. Bacteriol.* 197, 431–440. doi: 10.1128/JB.02282-14

Zhang, R., and Sharkey, T. D. (2009). Photosynthetic electron transport and proton flux under moderate heat stress. *Photosynth. Res.* 100, 29–43. doi: 10.1007/s11120-009-9420-8

Zhao, J., Hartmann, H., Trumbore, S., Ziegler, W., and Zhang, Y. (2013). High temperature causes negative whole-plant carbon balance under mild drought. *N. Phytol.* 200, 330–339. doi: 10.1111/nph.12400

Conflict of Interest Statement: The authors declare that the research was conducted in the absence of any commercial or financial relationships that could be construed as a potential conflict of interest.

Copyright © 2018 Birami, Gattmann, Heyer, Grote, Arneth and Ruehr. This is an open-access article distributed under the terms of the Creative Commons Attribution License (CC BY). The use, distribution or reproduction in other forums is permitted, provided the original author(s) and the copyright owner(s) are credited and that the original publication in this journal is cited, in accordance with accepted academic practice. No use, distribution or reproduction is permitted which does not comply with these terms.